



Photonic Reporting of Electrochemical Reactions Using Light-Emitting Diodes

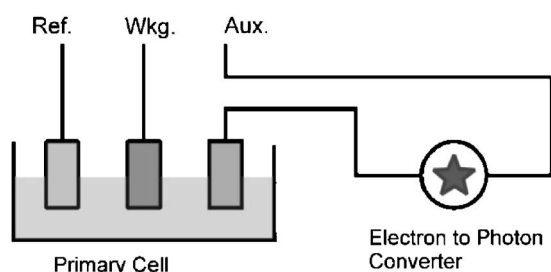
Li Sun and Richard M. Crooks*^z

Department of Chemistry, Texas A&M University, College Station, Texas 77842-3012, USA

The use of light-emitting diodes (LEDs) as photonic reporters of electrochemical reactions is examined and compared to an electron-to-photon conversion strategy involving electrogenerated chemiluminescence (ECL). The results indicate that it is possible to evaluate the rate of electrochemical reactions photonically without making direct current measurements. Compared to ECL, LED reporting has the following performance benefits: lower threshold current for photon emission, more efficient and stable electron-to-photon conversion, and larger dynamic range. Electrochemical reactions occurring in an array of ten thin-layer electrochemical cells are simultaneously evaluated using a corresponding array of LEDs.
© 2005 The Electrochemical Society. [DOI: 10.1149/1.2050367] All rights reserved.

Manuscript submitted May 9, 2005; revised manuscript received June 26, 2005. Available electronically October 4, 2005.

We describe here photonic reporting of electrochemical reactions using light-emitting diodes (LEDs). Scheme 1 illustrates the general



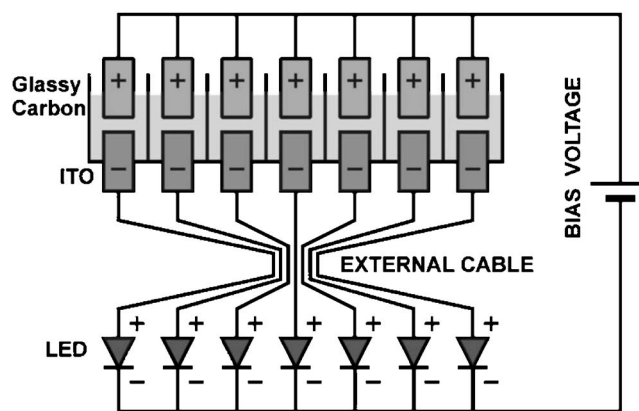
Scheme 1.

configuration used for this method. It consists of a conventional electrochemical cell connected in series with an electron-to-photon (EP) converter. The EP converter could be either an electrogenerated chemiluminescence (ECL)¹⁻³ cell or an LED. We focus here on the latter, because compared to ECL reporting LEDs have the following desirable attributes: (i) lower current threshold for photon emission, (ii) stable or time-independent EP conversion, (iii) slightly higher EP conversion efficiency, and (iv) larger dynamic range. In addition to using EP converters for individual electrochemical cells, we also show that an array of LEDs can be used to simultaneously report the current signals from many electrochemical cells. This is potentially important in microfluidics-based applications, because it eliminates the need for performing multiple current measurements simultaneously.

Electrochemical experiments often involve application of a potential to an electrode and measurement of the resulting current. This approach works well for single-cell experiments, but microfluidic-based electrochemical methods⁴⁻⁷ have opened up the possibility of fabricating tens or hundreds of electrochemical cells on a single chip and simultaneously carrying out an equivalent number of electrochemical reactions.⁸ In such cases, it is necessary to think about detecting the output of these cells in parallel. However, dc measurements become cumbersome at this scale, so a good alternative is to measure a photon flux that is proportional to the current. We previously addressed this issue by showing that ECL can be used as an indirect photonic reporter of current.⁹⁻¹¹ ECL detection is well-suited to the microfluidic environment, because a charge-coupled device (CCD) camera can be used to simultaneously measure the current output from multiple, densely packed cells on a single chip.

Moreover, there are some cases, such as those involving electrochemical reactions occurring at single (bipolar) electrodes,⁹ where it is impossible to make direct current measurements under any circumstances.

For the examples mentioned in the previous paragraph, the ECL reporting unit was an integral part of the microfluidic network. In contrast, the LED EP converters used in this study can be physically separated from the fluidics (Scheme 1). This makes it possible to independently optimize the electrochemical cell and the LED reporter. However, unlike ECL reporting, wires are required to connect each electrode in the array to the corresponding LED reporters. The presence of these wires brings up two questions regarding the potential advantages of LED reporting. First, it is clear that if the three-electrode configuration illustrated in Scheme 1 was expanded into an array format, then it would be necessary to independently control the potential of each electrode in parallel (multiple potentiostats) or in serial (via multiplexing). This would make LED reporting too complicated and thus defeat the original purpose of simplifying current measurements from electrochemical arrays. It is therefore obvious that two-electrode electrochemical cells are required to simplify the interconnection between electrochemical cells and LEDs. This is the approach we have adopted in this work (Scheme 2).



Scheme 2.

The second question concerns the possible advantage of LED reporting compared to simply making direct current measurements for each electrode in an array. At present, it is unclear which approach would be more advantageous for a particular application. This is mainly because there is little experimental work in the literature comparing LED and direct current measurements. We speculate that current measurements would be more efficient, because no

* Electrochemical Society Active Member.

^z E-mail: crooks@cm.utexas.edu

signal conversion (EP) is required. However, the LED approach is easier to implement, because both LEDs and CCD detectors are standard components that are readily available, and because the CCD readout is well-suited for handling data present in an array format.

The use of LEDs to measure the rates of electrochemical reactions was first reported by Faulkner and co-workers.^{12,13} Their motivation was to improve the time resolution for low-current electrochemical experiments. Unlike current measurements, which are relatively slow due to stray capacitance, photon measurements, such as time-correlated single-photon counting,^{14,15} can achieve nanosecond time resolution even for weak signals. However, the emphasis in this study is not to improve time resolution but to improve the EP conversion efficiency and other performance characteristics useful for microelectrochemical analyses. We wish to point out that the configuration we adopted (Scheme 1) is different from that of Faulkner and co-workers, who used the LED as a feedback resistor in the main amplifier of the potentiostat.¹³ In contrast, the LED shown in Scheme 1 is not part of the potentiostat circuit. Furthermore, we have chosen a thin-layer cell for electrochemical analysis, because this approach makes it possible to eliminate the reference electrode, eliminate the need for a potentiostat to control the bias voltage across the cell, and produce a steady-state photonic signal that is easier to measure than a transient signal.

In this study, we compare the performance characteristics of LED- and ECL-based EP converters. The results indicate that the EP conversion efficiency of the best LED is higher than that of the ECL cell. In addition, the LED efficiency is not a function of time, whereas the efficiency of the ECL cell depends on the mass-transport rate of the reactants responsible for light emission to the reporter electrode. A dual-cell configuration (Scheme 1) was used to illustrate the fundamental principles of LED-based reporting. The diffusion-limited steady-state current passing through the cell was found to be linearly proportional to the concentration of a model redox analyte, $K_3Fe(CN)_6$, and the magnitude of this current could be determined from the LED emission intensity because current and photon intensity have a one-to-one, or single-valued, functional relationship. Finally, a ten-element LED array was used to demonstrate simultaneous photonic reporting from ten thin-layer, two-electrode cells.

Experimental

Chemicals.— All solutions were prepared with deionized water (18 M Ω cm, Milli-Q, Millipore). $NaH_2PO_4 \cdot H_2O$ and $Na_2HPO_4 \cdot 7H_2O$ (Mallinckrodt), $K_3Fe(CN)_6$ (Fisher), NaCl (EM Science), and tripropylamine (TPA, 99+%) and $Ru(bpy)_3Cl_2 \cdot 6H_2O$ (bpy = bipyridine, 99.95%) from Aldrich were used as received. Phosphate buffer solutions (100 mM) contained a 5.57 molar ratio of HPO_4^{2-} to $H_2PO_4^-$, which yielded an empirical solution pH value of 7.5.¹⁶

ECL and LED performance comparison.— The LED used for performance comparison with ECL was a 5.0-mm-diam red emitter with peak wavelength of 660 nm (T1-3/4 package, 1.7 V typical forward bias, 30 mA maximum current, and 2800 mcd luminous intensity; SSL-LX5093SRC/E, Digi-Key, Thief River Falls, MN). The corresponding ECL cell was a three-electrode design. Figure 1a shows the schematic side view of the cell, which consisted of a 3-mm-thick poly(dimethylsiloxane) (PDMS)¹⁷ spacer (Sylgard 184, Dow Corning) sandwiched between a piece of Delrin plastic and a glass window. Prior to cell assembly, the Delrin piece was machined and press-fitted with a 1.0-mm-diam glassy carbon rod (Alfa Aesar), and then the Delrin surface, containing both the inlet/outlet ports and the glassy carbon disk, was mechanically polished successively with 600-grit (Buehler, Lake Bluff, IL), 5- μ m, and 3- μ m (Thorlab, Newton, NJ) sandpaper. An auxiliary electrode (0.25-mm diam and 4-cm long Pt/10% Ir wire, Sigmund Cohn, Mount Vernon, NY) and a Ag/AgCl reference electrode (made from a 0.25-mm-diam Ag wire, Alfa Aesar) were introduced into the cell by piercing the

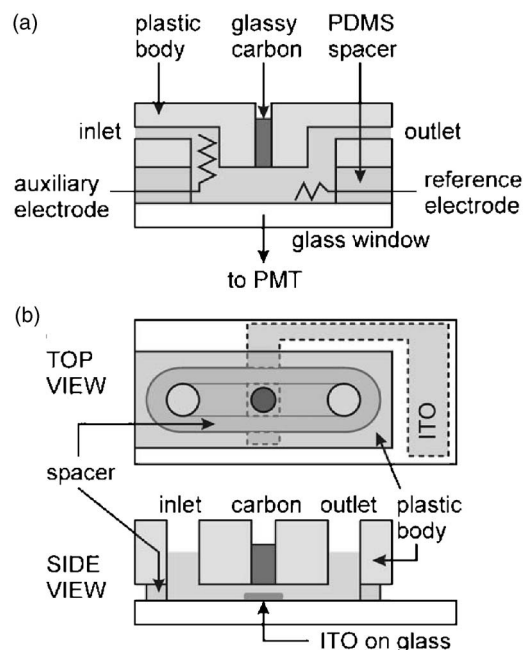


Figure 1. (a) Schematic illustration of the electrochemical cell used for studying the EP conversion efficiency of the ECL reporting principle. The working electrode is a 1.0-mm-diam glassy carbon disk, the auxiliary electrode is a coiled Pt/Ir wire, and the reference electrode is a Ag/AgCl wire. (b) Schematic illustrations of the thin-layer, dual-electrode cell used for the LED-reporting experiments. The cell allows steady-state concentration measurements of redox molecules cycling between the two electrodes. The anode is a 3.0-mm-diam glassy carbon disk, the cathode is a 4.0-mm-wide strip of ITO, and the spacer is made of 50- μ m-thick double-sided tape.

PDMS spacer with the wires. This ECL reporting cell, which had a volume of about 0.4 mL, was filled with an electrolyte solution containing 1.0 mM $Ru(bpy)_3Cl_2$, 10 mM TPA, 10 mM NaCl, and 100 mM pH 7.5 phosphate buffer solution. The NaCl was added to help stabilize the Ag/AgCl reference electrode, and potentials were referenced to this electrode without correction or calibration.

Cyclic voltammograms (CVs) of ECL reactions in the three-electrode cell were recorded using a computer-based potentiostat (model CHI750B potentiostat, CH Instruments, Austin, TX), and the ECL emission was quantified simultaneously using a photomultiplier tube (PMT) detector (model MP 953, Perkin Elmer, Santa Clara, CA) placed 7 mm from the glassy carbon electrode. To expand the dynamic range of the PMT, a neutral density filter (optical density = 1.0, Corion Corp, Holliston, MA) was sometimes used, and the measured light intensity was corrected accordingly. CVs and photoemission for the LED were characterized similarly, but without using the reference electrode.

LED reporting by an array of thin-layer electrochemical cells.— The device used for LED-based reporting consisted of ten identical thin-layer, two-electrode cells connected via external wires to an array of ten LEDs. Figure 1b illustrates the design of one electrochemical cell in the array of ten. The housing consisted of a 50- μ m-thick spacer, cut from 467MP double-sided tape (3M Co.) with a razor blade, sandwiched between a Delrin plastic body and a piece of glass supporting a patterned indium tin oxide (ITO) electrode^{9,18,19} (140-nm-thick ITO coating on 0.5-mm-thick Corning 1737 glass slide, Delta Technologies, Stillwater, MN). Inlet and outlet reservoirs (4.0 mm diam) were drilled into the Delrin body, and a glassy carbon electrode (3.0 mm diam) was integrated into the cell using the procedure described earlier for the ECL cell (Fig. 1a). The ITO electrode was patterned as a 4.0-mm-wide strip, and electrical contact was achieved using a spring-loaded, gold-coated pin (50F5583, Newark, Chicago, IL).

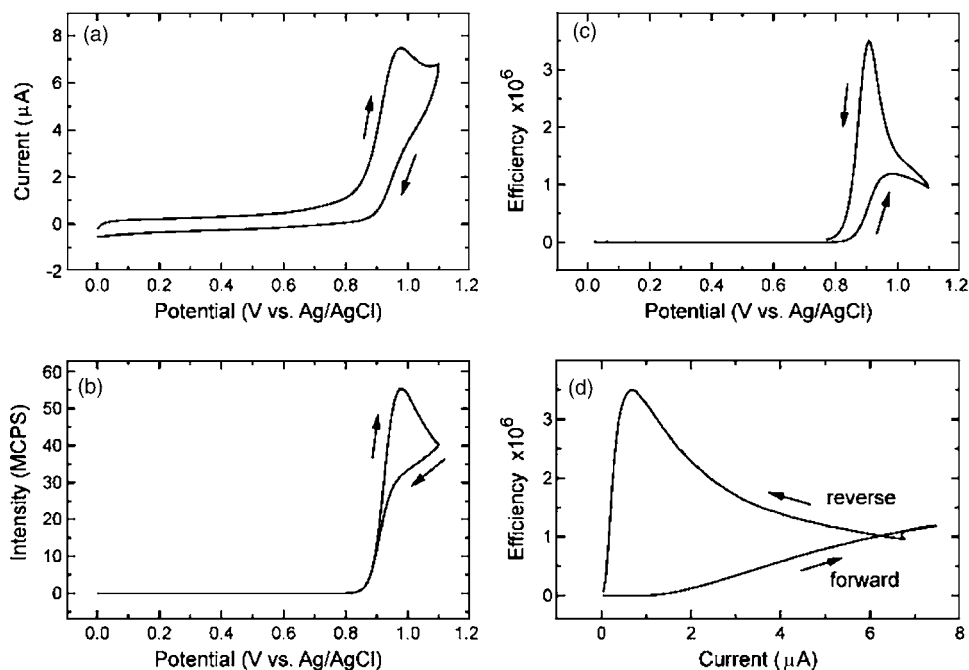


Figure 2. Characterization of the ECL EP converter using the cell shown in Fig. 1a. (a) CV obtained using a 1.0-mm-diam glassy carbon electrode in an electrolyte containing 1.0 mM $\text{Ru}(\text{bpy})_3\text{Cl}_2$, 10 mM TPA, 10 mM NaCl, and 100 mM pH 7.5 phosphate buffer. (b) Intensity of the ECL emission (MCPS = megacounts/s) from the glassy carbon electrode recorded concurrently with the CV in (a). The overall EP conversion efficiency (including the quantum yield of the PMT detector), ϕ , can be calculated according to Eq. 1, and is plotted here as a function of (c) the electrode potential and (d) the total current. Arrows pointing to the right indicate the forward potential scan, and the arrows pointing to the left indicate the reverse potential scan. The scan rate was 100 mV/s.

The LED array was connected to the array of electrochemical cells using external wires. It was fabricated from ten surface-mount red LEDs (660-nm peak emission, 10-mA forward current at 1.7-V bias, and 32-mcd luminous intensity; P596CT-ND, Digi-Key). These LEDs had less EP conversion efficiency than those used for the LED-ECL performance comparison discussed in the previous section, but they were smaller in size and thus more suitable for imaging with an optical microscope (vide infra). Electrical connection to the LEDs was achieved using a custom-designed printed-circuit board on which the LEDs were mounted using thermally cured Ag epoxy (H20E, Epoxy Technology, Billerica, MA).

The thin-layer electrochemical cells were characterized by chronoamperometry using the glassy carbon electrode as the anode and the ITO electrode as the cathode. The electrolyte solution (various concentrations of $\text{K}_3\text{Fe}(\text{CN})_6$ in 100 mM aqueous NaCl) was injected into the inlet of each cell with a 1-mL plastic syringe, which fit snugly to the inner wall of the inlet. The chronoamperometric experiments were carried out by applying a staircase waveform between the two electrodes, starting at 0 mV and increasing the bias by 200 mV every 30 s, and then measuring the steady-state current near the end of each 30-s period.

Photonic reporting from an array of electrochemical cells using an array of LEDs was carried out using the approach illustrated in Scheme 2. Each element of the array consisted of a forward-biased LED connected in series with a thin-layer electrochemical cell (Fig. 1b). A bias voltage was applied across all ten LED/thin-layer-cell units, and the emission from the LEDs was imaged using an inverted microscope (Eclipse TE300, Nikon). The LED array was projected via the top condenser lens of the microscope onto the sample stage as a reduced image ($2.2\times$ reduction), which was then captured via a 1x objective using a CCD camera (SenSys 1401E, Photometrics, Tucson, AZ).

Results and Discussion

Characterization of ECL and LED EP converters.— In ECL or LED reporting of electrochemical reactions, the current is conserved; that is, the current flowing through the EP converter (the ECL cell or the LED) is equal to the current flowing through the primary electrochemical cell. Under ideal conditions the current in the primary cell consists of only faradaic current, which in many electrochemical experiments is proportional to the analyte concentration.^{20,21} Under these conditions, the limit of detection

(LOD, in unit of concentration) for photonic reporting is determined largely by the current (threshold current) required to generate just enough light to be reliably distinguished from the dark noise of the photon detector (the photon detector signal when no current is passing through the EP converter). However, practical devices often deviate from this ideal situation, because the EP converter does not differentiate between faradaic and capacitive current. Moreover, faradaic background processes associated with the solvent, electrolyte, or impurities (e.g., oxygen) can also result in enough current to cause light emission from the EP converter even in the absence of the analyte. In other words, an analyte-free solution will likely produce a current that exceeds the EP threshold current. In such cases, the LOD will be determined not by the dark noise of the photon detector, but rather by the background current passing through the primary electrochemical cell.

It is clear from the foregoing discussion that measuring the functional relationship between the electrochemical current and the emitted light intensity is important for evaluating the performance characteristics of an EP converter. Figure 2a is a CV obtained in an aqueous solution containing $\text{Ru}(\text{bpy})_3^{2+}$ and TPA using the cell shown in Fig. 1a. The key features of the CV are an irreversible oxidation wave starting at about 0.8 V, corresponding to oxidation of TPA catalyzed by $\text{Ru}(\text{bpy})_3^{2+}$,¹⁻³ and a nonoverlapping loop at potentials less than 0.85 V, corresponding to the capacitive charging of the double layer.^{22,a} When the potential is larger than 0.85 V, a more substantial loop is also observed because of mass-transfer limitation of the ECL reagents to the electrode surface.

Figure 2b is a plot of ECL emission intensity as a function of potential that was concurrently recorded with the current/potential data shown in Fig. 2a. Unlike the electrochemical current, photon emission seems to be unaffected by the capacitive charging of the electrode double layer. That is, the forward and the reverse traces in Fig. 2b overlap (no loop) when the electrode potential is less than about 0.85 V. However, when the potential exceeds 0.85 V, the emission intensity traces (Fig. 2b) do exhibit a loop, similar to that in

^aThe capacitance of the glassy carbon electrode (1.0 mm diam), as determined from our CV data in an electrolyte containing 1 mM $\text{Ru}(\text{bpy})_3^{2+}$, 10 mM TPA, 10 mM NaCl, and 100 mM pH 7.5 phosphate buffer, is about $350 \mu\text{F}/\text{cm}^2$. This is comparable to $200 \mu\text{F}/\text{cm}^2$, a value inferred from the data reported by Wang et al. who used a 5.0-mm-diam glassy carbon to obtain CV in a 50 mM pH 7.4 phosphate buffer.

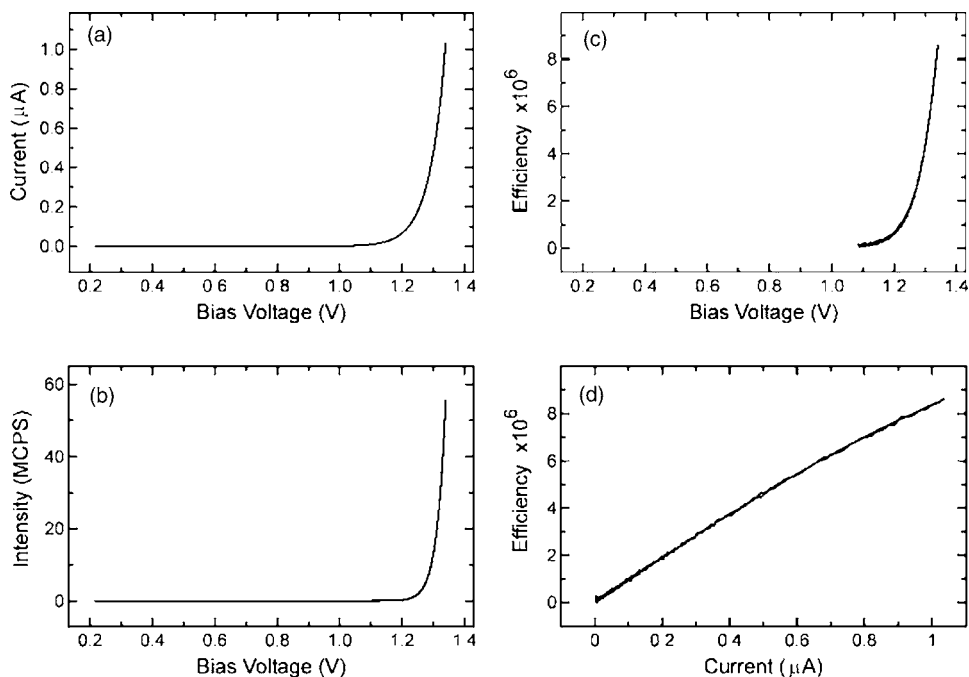


Figure 3. Characterization of an individual LED. Data were obtained by biasing the voltage between the two LED leads. (a) CV (i-V curve) of an LED under forward bias. (b) The intensity of LED emission recorded concurrently with the data shown in (a). The overall EP conversion efficiency (including the quantum yield of the PMT detector), ϕ , can be calculated according to Eq. 1, and is plotted as a function of (c) the bias voltage and (d) the current. The scan rate was 100 mV/s.

Fig. 2a, that arises from differences in concentrations or reaction rates of $\text{Ru}(\text{bpy})_3^{2+}/\text{TPA}$ at the electrode surface during the forward and reverse scans.^{2,23}

Figure 2c shows the overall EP conversion efficiency (including the quantum yield of the PMT detector), ϕ , corresponding to the data in Fig. 2a and b. ϕ is calculated according to Eq. 1

$$\phi = I/(i/e) = eI/i \quad [1]$$

Here e is the electron charge, i is the current, and I is the light intensity in units of counts per second (cps). It is clear from Fig. 2c that ϕ is not a single-valued function of the electrode potential but rather depends on the temporal history (scan direction) of the electrode polarization. This point is illustrated more clearly in Fig. 2d, which recasts the data in Fig. 2c to highlight the functional relationship between efficiency ϕ and current. A possible method for overcoming the time-dependent response is to generate ECL under time-independent, steady-state conditions. This could be achieved, for example, by flowing the $\text{Ru}(\text{bpy})_3^{2+}/\text{TPA}$ solution through the ECL cell and simultaneously flowing the analyte through the primary cell under steady state (constant flow velocity) conditions.^{10,11,24,25}

In addition to examining the performance characteristics of the ECL EP converter, we used the same methods to characterize a single LED EP converter. Figure 3a shows a CV obtained by linearly scanning the bias voltage across the two leads of the LED as a function of time, and Fig. 3b shows the simultaneously recorded light-emission intensity. Figures 3c and d are analogous to Fig. 2c and d. That is, Fig. 3c shows the EP conversion efficiency as a function of bias voltage, and Fig. 3d shows the EP conversion efficiency as a function of the current. In contrast to electrochemical cells, LEDs have negligible capacitance and therefore no loop structure is discernable in the LED CV data (compare Fig. 3a to Fig. 2a). In addition, photon emission from the LED recorded concurrently with the CV data also exhibits totally reversible behavior in that the forward and reverse traces overlay one another (compare Fig. 3b to Fig. 2b). This leads to several well-defined, single-valued relationships: for example, those between efficiency and bias voltage (Fig. 3c) and efficiency and current (Fig. 3d). These functional relationships are time-independent, because for LEDs both light emission

and electron conduction are steady-state processes that depend only on the bias voltage and not on time-dependent processes such as diffusion.

In addition to time-independent and highly stable EP conversion, LED reporting has other advantages compared to ECL. Comparison of Fig. 2d and Fig. 3d shows that the LED has a slightly higher EP conversion efficiency throughout the range of current displayed. In addition, LEDs require a lower threshold current (2 nA at 1.02 V bias voltage) to produce detectable light than ECL (400 nA at 0.66 V vs Ag/AgCl).^b As discussed in the beginning of this section, a lower threshold current is predicted to result in a lower LOD under ideal conditions. Finally, LEDs have a larger dynamic range for reporting current than the ECL system. The maximum current is about 7 μA for the particular ECL configuration used here. In contrast, the LED used to obtain the data shown in Fig. 3 is rated for a maximum current of 30 mA. The large dynamic range in current does not necessarily translate into a large dynamic range in analyte concentration (vide infra), because the LED emission varies nonlinearly with respect to the current.

LED reporting of an array of electrochemical reactions.—In the previous section we showed that there are several advantages of LED EP converters compared to ECL EP converters. However, for most applications it is more straightforward to simply measure faradaic current, and therefore it is necessary to establish a need for photonic reporting of electrochemical processes. For example, we have previously shown that ECL reporting provides a convenient means for measuring current in single-electrode cells.⁹ Neither direct measurement of faradaic current, nor LED-based measurements of the type describe here, are possible in this type of cell configuration.

The utility of LED-based reporting lies beyond the good performance characteristics mentioned earlier. For example, in this section we show how LEDs can be used to simultaneously report the current output from an array of electrochemical cells without the necessity

^bThe threshold current is defined as the current at which the signal to noise (S/N) ratio for photon emission detection is equal to 3.

of making multiple, simultaneous direct current measurements. Accordingly, this approach might find applications requiring large-scale screening of electrochemical processes.²⁶⁻²⁸

Thin-layer, two-electrode electrochemical cells were chosen to construct a prototype device that can simultaneously support up to ten electrochemical reactions. In addition to their compact size, two-electrode, thin-layer cells also simplify device design, because no reference electrode is required; produce a steady-state response that should be easier to detect than a transient signal; and even amplify the signal if a redox-active analyte can be recycled many times between the two narrowly spaced electrodes.²⁹ Interdigitated electrode arrays have a similar set of properties and could be used in place of the array of thin-layer cells.^{30,31}

According to Eq. 2, the current, i , passing through a thin-layer cell is linearly proportional to the analyte concentration^{32,33}

$$i = nFDAC/\delta = gC \quad [2]$$

Here n is the number of charges transferred per redox molecule; F is the Faraday constant; D is the effective diffusion coefficient;^c A is the overlapped area of the two electrodes that form the thin layer;^c C is the concentration; δ is the thickness of the cell if redox recycling between the two electrodes is purely diffusion-limited;^{29,32} and g , which can be thought of as a geometric cell constant, is equal to $nFDA/\delta$. To achieve diffusion-limited transport in a thin-layer cell, the bias voltage must be sufficient to drive the surface concentrations of the redox reactants to zero at both electrodes. Figure 4a shows the steady-state current as a function of the bias voltage for a single thin-layer cell containing 4.0 mM $K_3Fe(CN)_6$ and 100 mM NaCl. The data in Fig. 4a were collected using multipotential-step chronoamperometry, which was described in the Experimental section. When the bias is larger than 1.4 V, the steady-state current reaches a diffusion-limited value and remains approximately constant until the onset of solvent electrolysis at biases $> \sim 2.0$ V.

Figure 4b shows that there is a linear relationship between the diffusion-limited, steady-state current and the concentration of $K_3Fe(CN)_6$. The slope of this line, $10.5 \mu A/mM$, is the experimentally determined value of the geometric cell constant, g , mentioned earlier. This differs only slightly with the value of g calculated using Eq. 2: $9.4 \mu A/mM$. The discrepancy is likely caused by inaccurate control of the thickness of the thin-layer cell, which is determined by the thickness of the gasket separating the two electrodes. As a consequence, each thin-layer cell in the array has a different g value. When the ten cells were filled with 1.0 mM $K_3Fe(CN)_6$ and 100 mM NaCl, the average steady-state current was found to be $10.9 \pm 2.6 \mu A$ at a bias voltage of 1.5 V. This average steady-state current may be taken as a rough estimate of the average cell constant (in units of $\mu A/mM$).

Figure 5a is a micrograph of the light emission from the ten-element LED array. Each LED is connected to one of the ten thin-layer electrochemical cells, each of which contains 100 mM NaCl and either 0, 1.0, or 2.0 mM $K_3Fe(CN)_6$. Qualitatively, the intensity pattern agrees with the expectation that cells containing more concentrated $K_3Fe(CN)_6$ result in more emission intensity from the corresponding LEDs. The results can also be quantitatively evaluated. For any LED/thin-layer-cell unit, the concentration can be found by combining Eq. 1 and 2 to obtain Eq. 3, where k is the cell index

$$C_k = eI_k/(\varphi_k g_k) \quad [3]$$

Equation 3 shows that the concentration in a thin-layer cell can be calculated from the emission intensity once the EP conversion efficiency, φ , for the LED, and the corresponding cell constant, g , are known. Note that φ can be easily determined from plots of the sort

^cThe effective diffusion coefficient is $2 * D_O * D_R / (D_O + D_R)$, where D_O and D_R are the diffusion coefficients of the oxidized and reduced species, respectively. For the ferricyanide/ferrocyanide redox couple, $D_O = 7.20 \times 10^{-6}$ and $D_R = 6.66 \times 10^{-6}$. The projected electrode area, A , for this study is equal to the area of the 3-mm-diam glassy carbon anode, or 7.07 mm^2 .

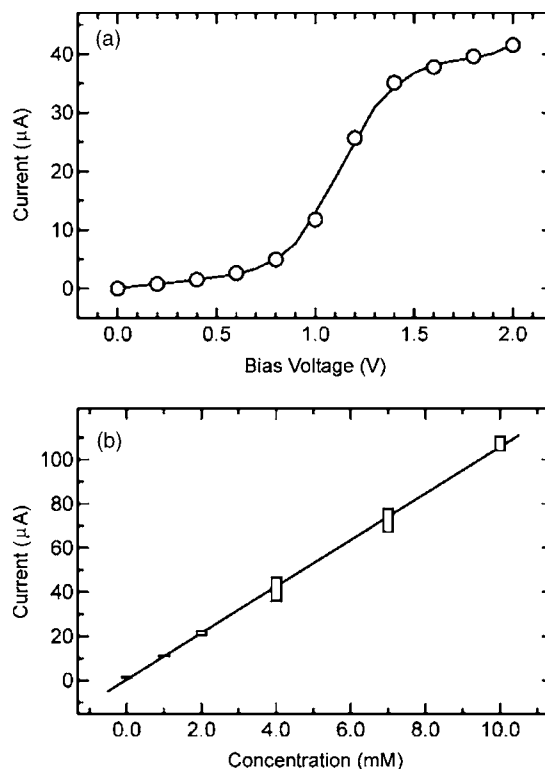


Figure 4. (a) Steady-state current as a function of bias voltage across a thin-layer, dual-electrode cell (Fig. 1b) containing 4.0 mM $K_3Fe(CN)_6$ and 100 mM NaCl. The steady-state current was measured after the bias voltage was applied for 30 s. The circles represent experimentally determined data, and the line is an empirical polynomial fit. (b) Diffusion-limited, steady-state current (obtained at a bias of 2.0 V) as a function of $K_3Fe(CN)_6$ concentration. The height of each rectangular bar represents the spread in the data (2σ) resulting from several measurements. The line is the least-squares fit to the data. The slope of this line, $10.5 \mu A/mM$, is comparable to the value calculated according to Eq. 2 ($9.4 \mu A/mM$).

shown in Fig. 3, because of the single-valued relationship between the emission intensity, the bias voltage, and the conversion efficiency. In addition, φ and g can be characterized and optimized separately because the LED array and the electrochemical array are independent units that have independent performance characteristics.

The quantification procedure described in the previous paragraph contains the assumption that the current passing through the thin-layer cell is diffusion-limited, and that it is relatively insensitive to slight changes in the bias voltage. Figure 5b illustrates this point by comparing the current-voltage curves of a representative thin-layer cell and companion LED. Because the thin-layer cell and the corresponding LED reporter are connected in series (Scheme 2), the total applied bias voltage (V_{TOTAL}) is equal to the sum of the individual voltages across the thin-layer cell (V_{TL}) and across the LED (V_{LED}): $V_{TOTAL} = V_{TL} + V_{LED}$. If V_{TOTAL} is kept constant, then V_{TL} will depend slightly on the total current passing through the cell, because V_{LED} is a weak function of this current.^d However, the i - v curve (or CV) of the LED has a near-vertical slope at biases > 1.4 V, which means that the change in V_{TL} will be small even when the current changes significantly. It follows that the total current passing through the device will remain approximately constant as long as V_{TL} lies within the range where the steady-state current is driven at the diffusion-limited rate.

^dBecause the current is proportional to the analyte concentration, the bias voltage (V_{TL}) across the thin-layer cell is also a function of concentration.

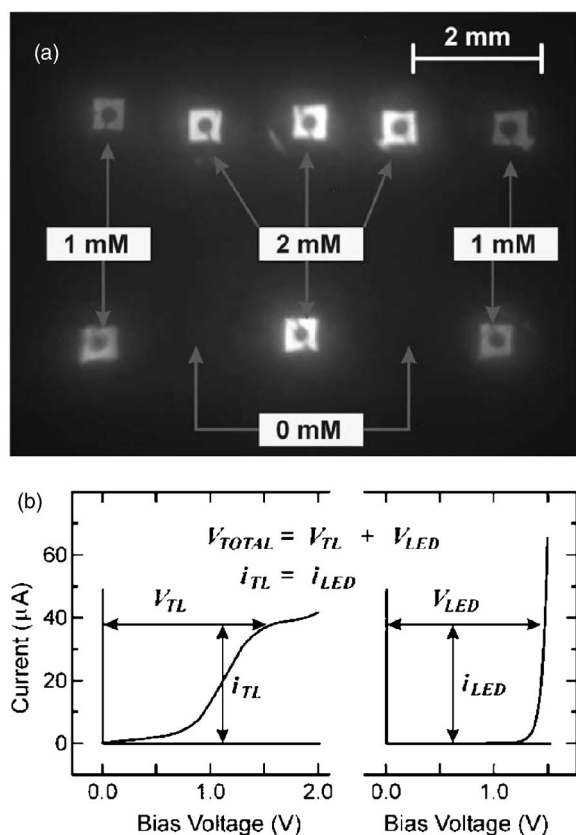


Figure 5. (a) Emission image (1315×1034 pixels; full gray scale: 0–2500 counts) obtained from a ten-element LED array that reports the current from an array of ten electrochemical thin-layer (TL) cells (Scheme 2). The $\text{K}_3\text{Fe}(\text{CN})_6$ concentration in each thin-layer cell is indicated. (b) The current passing through each thin-layer electrochemical cell is conserved: $i_{\text{TL}} = i_{\text{LED}}$. The total applied bias voltage (V_{TOTAL}) was 2.9 V, which is the sum of the bias voltages across the LED ($V_{\text{LED}} = \sim 1.4$ V) and the thin-layer cell ($V_{\text{TL}} = \sim 1.5$ V). If V_{TL} lies within the range where the steady-state current is driven at the diffusion-limited rate, then the LED emission intensity can be used to find the value for the steady-state current (from a plot similar to Fig. 3d), which can, in turn, be used to find the analyte concentration.

The experimentally determined and actual (in parentheses) concentrations for the cells shown in Fig. 5a, starting from the upper left corner of the image, are: 1.4 mM (1.0 mM, first row), 2.2 mM (2.0 mM), 2.2 mM (2.0 mM), 2.5 mM (2.0 mM), 1.0 mM (1.0 mM), 1.2 mM (1.0 mM, second row), 0.2 mM (0 mM), 1.9 mM (2.0 mM), 0.9 mM (0 mM), and 1.1 mM (1.0 mM). The relatively large errors for these data arise from a variety of sources. First, the calibration data for the LEDs (that is, the function ϕ) change over the course of several hours, probably because of temperature fluctuations.³⁴ Second, the cell constants gradually decrease after prolonged application of the bias voltage. This may be a consequence of progressive solution or electrode fouling. Finally, there might be some optical cross talk between neighboring LEDs, which can be coupled through the plastic lenses encapsulating the LED chips. For example, one cell that should have reported 0 mM analyte indicated a concentration of 0.9 mM. This indicates a higher than expected LED emission for that cell, which could be accounted for by coupling of light from the nearby bright LED. The relative error caused by this cross talk depends on the EP conversion efficiency of a particular LED. For example, stray light caused a relatively large error in the above example of LED reporting (0.9 mM reported value vs 0 mM actual value) than a similar more efficient LED on the left (0.2 mM reported value vs 0 mM actual value). That is, at a given current, the 0.9 mM LED emits less light than the 0.2-mM LED. It follows that,

at a given level of stray light, the 0.9-mM LED is more prone to the cross-talk interference than the 0.2 mM LED. We view the above limitations of the present system as engineering challenges that can be resolved after further development.

Conclusions

In summary, we have described a means for measuring the rates of electrochemical reactions using an LED as the EP converter. This approach requires that the photonic reporting unit (i.e., the LED) be separated from the electrochemical unit, which makes it possible to independently optimize the performance of each. Quantitative evaluation of both an LED EP converter and an ECL EP converter indicates that the LED has the following performance advantages: lower limit of detection, higher EP conversion efficiency, more stable response, and larger dynamic range. However, unlike ECL EP converters, LEDs cannot be coupled directly to an electrochemical reaction in a single electrolytic cell. Thus, LED reporting cannot completely substitute for ECL reporting in some cases, such as those involving electrochemical reactions occurring in single-electrode cells.^{9,10}

A significant outcome of this study is that it is possible to use an array of LEDs to simultaneously report electrochemical processes in ten thin-layer electrochemical cells. The ability to monitor multiple electrochemical reactions simultaneously, without the need for a potentiostat, current measurement system, or reference electrode, may render this approach useful for array-based sensing and combinatorial screening applications.

Acknowledgments

Financial support of this work was provided by the U.S. Army Medical Research and Materiel Command and the Texas Institute for Intelligent Bio-Nano Materials and Structures for Aerospace Vehicles, funded by NASA Cooperative Agreement No. NCC-1-02038. We thank Dr. William M. Lackowski for providing valuable information about the LEDs used in this work. We also thank Professor Allen J. Bard (University of Texas, Austin) for bringing to our attention related studies carried out by Dr. Larry R. Faulkner (University of Texas, Austin) in the mid-1980s, and Dr. Faulkner for providing a very useful doctoral dissertation.

Texas A&M University assisted in meeting the publication costs of this article.

References

1. M. M. Richter, *Chem. Rev. (Washington, D.C.)*, **104**, 3003 (2004).
2. Y. Zu and A. J. Bard, *Anal. Chem.*, **72**, 3223 (2000).
3. W. Miao, J.-P. Choi, and A. J. Bard, *J. Am. Chem. Soc.*, **124**, 14478 (2002).
4. N. J. Ronkainen-Matsuno, J. H. Thomas, H. B. Halsall, and W. R. Heineman, *Trends Anal. Chem.*, **21**, 213 (2002).
5. J. Rossier, F. Reymond, and P. E. Michel, *Electrophoresis*, **23**, 858 (2002).
6. W. R. Vandaveer IV, S. A. Pasas, R. S. Martin, and S. M. Lunte, *Electrophoresis*, **23**, 3667 (2002).
7. J. Wang, *Talanta*, **56**, 223 (2002).
8. W. Zhan and R. M. Crooks, *J. Am. Chem. Soc.*, **125**, 9934 (2003).
9. W. Zhan, J. Alvarez, and R. M. Crooks, *J. Am. Chem. Soc.*, **124**, 13265 (2002).
10. W. Zhan, J. Alvarez, and R. M. Crooks, *Anal. Chem.*, **75**, 313 (2003).
11. W. Zhan, J. Alvarez, L. Sun, and R. M. Crooks, *Anal. Chem.*, **75**, 1233 (2003).
12. L. R. Faulkner, P. He, D. Ingersoll, H.-J. Huang, and M. R. Walsh, in *Ultramicroelectrodes*, M. Fleisemann, B. S. Pons, D. R. Rolison, and P. P. Schmidt, Editors, pp. 225–239, Datatech, Morganton, NC (1987).
13. L. R. Faulkner, M. R. Walsh, and C. Xu, in *Contemporary Electroanalytical Chemistry*, A. Ivaska, A. Lewenstam, and R. Sara, Editors, pp. 5–14, Plenum Press, New York (1990).
14. F. V. Bright and C. A. Munson, *Anal. Chim. Acta*, **500**, 71 (2003).
15. G. Hungerford and D. J. S. Birch, *Meas. Sci. Technol.*, **7**, 121 (1996).
16. R. J. Beynon and J. S. Easterby, *Buffer Solutions: The Basics*, BIOS Scientific, Oxford (1996).
17. D. C. Duffy, J. C. McDonald, O. J. A. Schueller, and G. M. Whitesides, *Anal. Chem.*, **70**, 4974 (1998).
18. J.-H. Lan, J. Kanicki, A. Catalano, J. Keane, W. Den Boer, and T. Gu, *J. Electron. Mater.*, **25**, 1806 (1996).
19. M. Scholten and J. E. A. M. van den Meerakker, *J. Electrochem. Soc.*, **140**, 471 (1993).
20. A. J. Bard and L. R. Faulkner, *Electrochemical Methods, Fundamentals and Applications*, Wiley, New York (1980).
21. P. T. Kissinger and W. R. Heineman, *Laboratory Techniques in Electroanalytical Chemistry*, 2nd ed., Marcel Dekker, New York (1996).
22. J. Wang, T. Martinez, D. R. Yaniv, and L. D. McCormick, *J. Electroanal. Chem.*

- Interfacial Electrochem.*, **278**, 379 (1990).
23. Y. Zu and A. J. Bard, *Anal. Chem.*, **73**, 3960 (2001).
 24. A. Arora, A. J. de Mello, and A. Manz, *Anal. Commun.*, **34**, 393 (1997).
 25. R. G. Compton, A. C. Fisher, R. G. Wellington, P. J. Dobson, and P. A. Leigh, *J. Phys. Chem.*, **97**, 10410 (1993).
 26. E. Reddington, A. Sapienza, B. Gurau, R. Viswanathan, S. Sarangapani, E. S. Smotkin, and T. E. Mallouk, *Science*, **280**, 1735 (1998).
 27. A. J. Ricco, T. D. Boone, Z. H. Fan, I. Gibbons, T. Matray, S. Singh, H. Tan, T. Tian, and S. J. Williams, *Biochem. Soc. Trans.*, **30**, 73 (2002).
 28. J. R. Schullek, J. H. Butler, Z.-J. Ni, D. Chen, and Z. Yuan, *Anal. Biochem.*, **246**, 20 (1997).
 29. J. Kwak and A. J. Bard, *Anal. Chem.*, **61**, 1221 (1989).
 30. O. Niwa, Y. Xu, H. B. Halsall, and W. R. Heineman, *Anal. Chem.*, **65**, 1559 (1993).
 31. D. Liu, R. K. Perdue, L. Sun, and R. M. Crooks, *Langmuir*, **20**, In press (2004).
 32. L. B. Anderson and C. N. Reilley, *J. Electroanal. Chem. Interfacial Electrochem.*, **10**, 538 (1965).
 33. S. J. Konopka and B. McDuffie, *Anal. Chem.*, **42**, 1741 (1970).
 34. V. Vilokinen, P. Sipila, P. Melanen, M. Saarinen, S. Orsila, M. Dumitrescu, P. Savolainen, M. Toivonen, and M. Pessa, *Mater. Sci. Eng., B*, **74**, 165 (2000).